

### 3.15 LIFTING FLOW OVER A CYLINDER

In Section 3.13, we superimposed a uniform flow and a doublet to synthesize the flow over a circular cylinder, as shown in Figure 3.26. In addition, we proved that both the lift and drag were zero for such a flow. However, the streamline pattern shown at the right of Figure 3.26 is not the only flow that is theoretically possible around a circular cylinder. It is the only flow that is consistent with zero lift. However, there are other possible flow patterns around a circular cylinder—different flow patterns that result in a nonzero lift on the cylinder. Such lifting flows are discussed in this section.

Now you might be hesitant at this moment, perplexed by the question as to how a lift could possibly be exerted on a circular cylinder. Is not the body perfectly symmetric, and would not this geometry always result in a symmetric flow field with a consequent zero lift, as we have already discussed? You might be so perplexed that you run down to the laboratory, place a stationary cylinder in a low-speed tunnel, and measure the lift. To your satisfaction, you measure no lift, and you walk away muttering that the subject of this section is ridiculous—there is no lift on the cylinder. However, go back to the wind tunnel, and this time run a test with the cylinder *spinning* about its axis at relatively high revolutions per minute. This time you measure a *finite* lift. Also, by this time you might be thinking of other situations: spin on a baseball causes it to curve, and spin on a golfball causes it to hook or slice. Clearly, in real life there are nonsymmetric aerodynamic forces acting on these symmetric, spinning bodies. So, maybe the subject matter of this section is not so ridiculous after all. Indeed, as you will soon appreciate, the concept of lifting flow over a cylinder will start us on a journey which leads directly to the theory of the lift generated by airfoils, as discussed in Chapter 4.

Consider the flow synthesized by the addition of the nonlifting flow over a cylinder and a vortex of strength  $\Gamma$ , as shown in Figure 3.32. The stream function

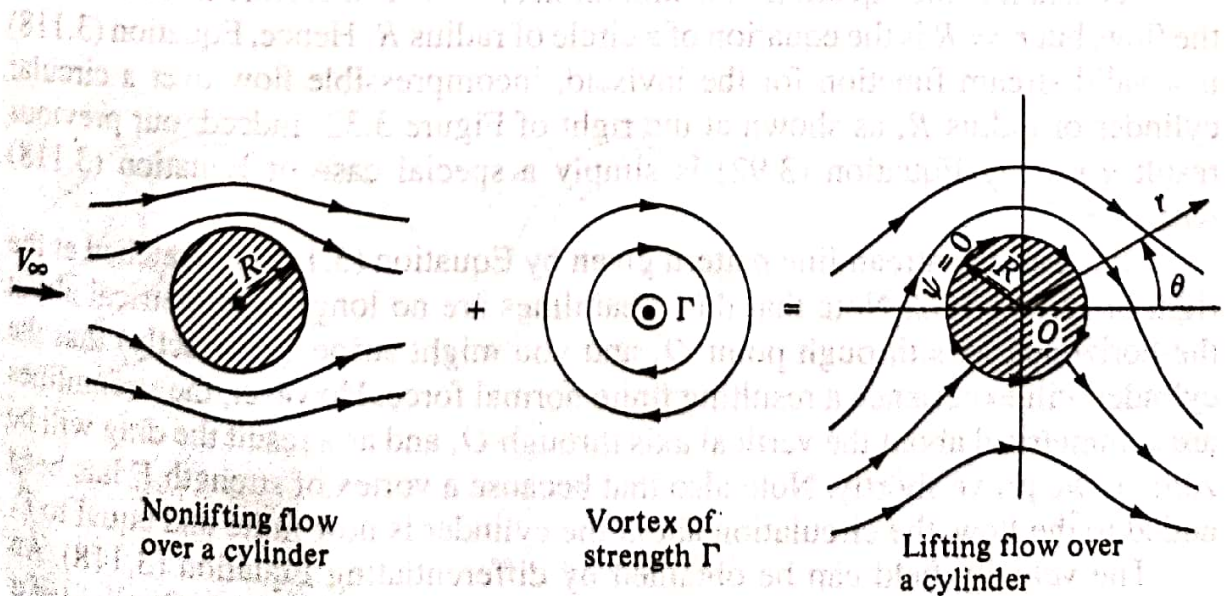


Figure 3.32 The synthesis of lifting flow over a circular cylinder.

for nonlifting flow over a circular cylinder of radius  $R$  is given by Equation (3.92):

$$\psi_1 = (V_\infty r \sin \theta) \left( 1 - \frac{R^2}{r^2} \right) \quad (3.92)$$

The stream function for a vortex of strength  $\Gamma$  is given by Equation (3.114). Recall that the stream function is determined within an arbitrary constant; hence, Equation (3.114) can be written as

$$\psi_2 = \frac{\Gamma}{2\pi} \ln r + \text{const} \quad (3.115)$$

Since the value of the constant is arbitrary, let

$$\text{Const} = -\frac{\Gamma}{2\pi} \ln R \quad (3.116)$$

Combining Equations (3.115) and (3.116), we obtain

$$\psi_2 = \frac{\Gamma}{2\pi} \ln \frac{r}{R} \quad (3.117)$$

Equation (3.117) is the stream function for a vortex of strength  $\Gamma$  and is just as valid as Equation (3.114) obtained earlier; the only difference between these two equations is a constant of the value given by Equation (3.116).

The resulting stream function for the flow shown at the right of Figure 3.32 is

$$\psi = \psi_1 + \psi_2$$

or

$$\boxed{\psi = (V_\infty r \sin \theta) \left( 1 - \frac{R^2}{r^2} \right) + \frac{\Gamma}{2\pi} \ln \frac{r}{R}} \quad (3.118)$$

From Equation (3.118), if  $r = R$ , then  $\psi = 0$  for all values of  $\theta$ . Since  $\psi = \text{constant}$  is the equation of a streamline,  $r = R$  is therefore a streamline of the flow, but  $r = R$  is the equation of a circle of radius  $R$ . Hence, Equation (3.118) is a valid stream function for the inviscid, incompressible flow over a circular cylinder of radius  $R$ , as shown at the right of Figure 3.32. Indeed, our previous result given by Equation (3.92) is simply a special case of Equation (3.118) with  $\Gamma = 0$ .

The resulting streamline pattern given by Equation (3.118) is sketched at the right of Figure 3.32. Note that the streamlines are no longer symmetrical about the horizontal axis through point  $O$ , and you might suspect (correctly) that the cylinder will experience a resulting finite normal force. However, the streamlines are symmetrical about the vertical axis through  $O$ , and as a result the drag will be zero, as we prove shortly. Note also that because a vortex of strength  $\Gamma$  has been added to the flow, the circulation about the cylinder is now finite and equal to  $\Gamma$ .

The velocity field can be obtained by differentiating Equation (3.118). An equally direct method of obtaining the velocities is to add the velocity field of a vortex to the velocity field of the nonlifting cylinder. (Recall that because of the linearity of the flow, the velocity components of the superimposed elementary

flows add directly.) Hence, from Equations (3.93) and (3.94) for nonlifting flow over a cylinder of radius  $R$ , and Equations (3.111a and b) for vortex flow, we have, for the lifting flow over a cylinder of radius  $R$ ,

$$V_r = \left(1 - \frac{R^2}{r^2}\right) V_\infty \cos \theta \quad (3.119)$$

$$V_\theta = -\left(1 + \frac{R^2}{r^2}\right) V_\infty \sin \theta - \frac{\Gamma}{2\pi r} \quad (3.120)$$

To locate the stagnation points in the flow, set  $V_r = V_\theta = 0$  in Equations (3.119) and (3.120) and solve for the resulting coordinates  $(r, \theta)$ :

$$V_r = \left(1 - \frac{R^2}{r^2}\right) V_\infty \cos \theta = 0 \quad (3.121)$$

$$V_\theta = -\left(1 + \frac{R^2}{r^2}\right) V_\infty \sin \theta - \frac{\Gamma}{2\pi r} = 0 \quad (3.122)$$

From Equation (3.121),  $r = R$ . Substituting this result into Equation (3.122) and solving for  $\theta$ , we obtain

$$\theta = \arcsin\left(-\frac{\Gamma}{4\pi V_\infty R}\right) \quad (3.123)$$

Since  $\Gamma$  is a positive number, from Equation (3.123)  $\theta$  must be in the third and fourth quadrants. That is, there can be two stagnation points on the bottom half of the circular cylinder, as shown by points 1 and 2 in Figure 3.33a. These points are located at  $(R, \theta)$ , where  $\theta$  is given by Equation (3.123). However, this result is valid only when  $\Gamma/4\pi V_\infty R < 1$ . If  $\Gamma/4\pi V_\infty R > 1$ , then Equation (3.123) has no meaning. If  $\Gamma/4\pi V_\infty R = 1$ , there is only one stagnation point on the surface of the cylinder, namely, point  $(R, -\pi/2)$  labeled as point 3 in Figure 3.33b. For

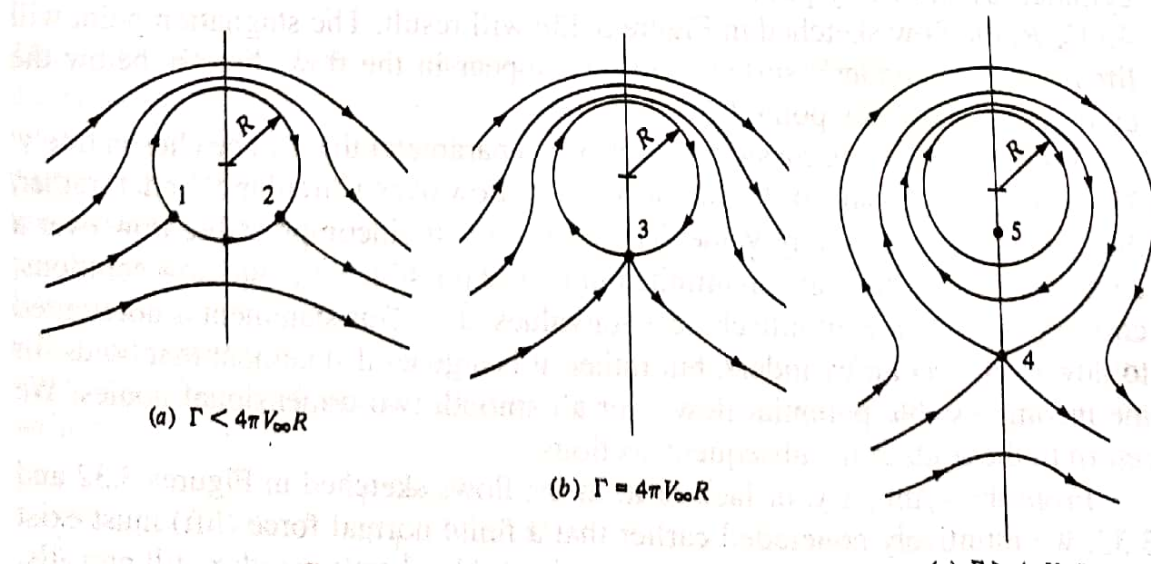


**Figure 3.33** Stagnation points for the lifting flow over a circular cylinder.

the case of  $\Gamma/4\pi V_\infty R > 1$ , return to Equation (3.121). We saw earlier that it is satisfied by  $r = R$ ; however, it is also satisfied by  $\theta = \pi/2$  or  $-\pi/2$ . Substituting  $\theta = -\pi/2$  into Equation (3.122), and solving for  $r$ , we have

$$r = \frac{\Gamma}{4\pi V_\infty} \pm \sqrt{\left(\frac{\Gamma}{4\pi V_\infty}\right)^2 - R^2} \quad (3.124)$$

Hence, for  $\Gamma/4\pi V_\infty R > 1$ , there are two stagnation points, one inside and the other outside the cylinder, and both on the vertical axis, as shown by points 4 and 5 in Figure 3.33c. [How does one stagnation point fall *inside* the cylinder? Recall that  $r = R$ , or  $\psi = 0$ , is just one of the allowed streamlines of the flow. There is a theoretical flow inside the cylinder—flow that is issuing from the doublet at the origin superimposed with the vortex flow for  $r < R$ . The circular streamline  $r = R$  is the dividing streamline between this flow and the flow from the freestream. Therefore, as before, we can replace the dividing streamline by a solid body—our circular cylinder—and the *external* flow will not know the difference. Hence, although one stagnation point falls inside the body (point 5), we are not realistically concerned about it. Instead, from the point of view of flow over a solid cylinder of radius  $R$ , point 4 is the only meaningful stagnation point for the case  $\Gamma/4\pi V_\infty R > 1$ .]

The results shown in Figure 3.33 can be visualized as follows. Consider the inviscid incompressible flow of given freestream velocity  $V_\infty$  over a cylinder of given radius  $R$ . If there is no circulation (i.e., if  $\Gamma = 0$ ), the flow is given by the sketch at the right of Figure 3.26, with horizontally opposed stagnation points *A* and *B*. Now assume that a circulation is imposed on the flow, such that  $\Gamma < 4\pi V_\infty R$ . The flow sketched in Figure 3.33a will result; the two stagnation points will move to the lower surface of the cylinder as shown by points 1 and 2. Assume that  $\Gamma$  is further increased until  $\Gamma = 4\pi V_\infty R$ . The flow sketched in Figure 3.33b will result, with only one stagnation point at the bottom of the cylinder, as shown by point 3. When  $\Gamma$  is increased still further such that  $\Gamma > 4\pi V_\infty R$ , the flow sketched in Figure 3.33c will result. The stagnation point will lift from the cylinder's surface and will appear in the flow directly below the cylinder, as shown by point 4.

From the above discussion,  $\Gamma$  is clearly a parameter that can be chosen freely. There is no single value of  $\Gamma$  that “solves” the flow over a circular cylinder; rather, the circulation can be any value. Therefore, for the incompressible flow over a circular cylinder, there are an infinite number of possible potential flow solutions, corresponding to the infinite choices for values of  $\Gamma$ . This statement is not limited to flow over circular cylinders, but rather, it is a general statement that holds for the incompressible potential flow over all smooth two-dimensional bodies. We return to these ideas in subsequent sections.

From the symmetry, or lack of it, in the flows sketched in Figures 3.32 and 3.33, we intuitively concluded earlier that a finite normal force (lift) must exist on the body but that the drag is zero; that is, d'Alembert's paradox still prevails. Let us quantify these statements by calculating expressions for lift and drag, as follows.

The velocity on the surface of the cylinder is given by Equation (3.120) with  $r = R$ :

$$V = V_\theta = -2V_\infty \sin \theta - \frac{\Gamma}{2\pi R} \quad (3.125)$$

In turn, the pressure coefficient is obtained by substituting Equation (3.125) into Equation (3.38):

$$\begin{aligned} C_p &= 1 - \left( \frac{V}{V_\infty} \right)^2 = 1 - \left( -2 \sin \theta - \frac{\Gamma}{2\pi RV_\infty} \right)^2 \\ \text{or } C_p &= 1 - \left[ 4 \sin^2 \theta + \frac{2\Gamma \sin \theta}{\pi RV_\infty} + \left( \frac{\Gamma}{2\pi RV_\infty} \right)^2 \right] \end{aligned} \quad (3.126)$$

In Section 1.5, we discussed in detail how the aerodynamic force coefficients can be obtained by integrating the pressure coefficient and skin friction coefficient over the surface. For inviscid flow,  $c_f = 0$ . Hence, the drag coefficient  $c_d$  is given by Equation (1.16) as

$$\begin{aligned} c_d &= c_a = \frac{1}{c} \int_{LE}^{TE} (C_{p,u} - C_{p,l}) dy \\ \text{or } c_d &= \frac{1}{c} \int_{LE}^{TE} C_{p,u} dy - \frac{1}{c} \int_{LE}^{TE} C_{p,l} dy \end{aligned} \quad (3.127)$$

Converting Equation (3.127) to polar coordinates, we note that

$$y = R \sin \theta \quad dy = R \cos \theta d\theta \quad (3.128)$$

Substituting Equation (3.128) into (3.127), and noting that  $c = 2R$ , we have

$$c_d = \frac{1}{2} \int_{\pi}^0 C_{p,u} \cos \theta d\theta - \frac{1}{2} \int_{\pi}^{2\pi} C_{p,l} \cos \theta d\theta \quad (3.129)$$

The limits of integration in Equation (3.129) are explained as follows. In the first integral, we are integrating from the leading edge (the front point of the cylinder), moving over the *top* surface of the cylinder. Hence,  $\theta$  is equal to  $\pi$  at the leading edge and, moving over the top surface, *decreases* to 0 at the trailing edge. In the second integral, we are integrating from the leading edge to the trailing edge while moving over the *bottom* surface of the cylinder. Hence,  $\theta$  is equal to  $\pi$  at the leading edge and, moving over the bottom surface, *increases* to  $2\pi$  at the trailing edge. In Equation (3.129), both  $C_{p,u}$  and  $C_{p,l}$  are given by the same analytic expression for  $C_p$ , namely, Equation (3.126). Hence, Equation (3.129) can be written as

$$\begin{aligned} c_d &= -\frac{1}{2} \int_0^\pi C_p \cos \theta d\theta - \frac{1}{2} \int_\pi^{2\pi} C_p \cos \theta d\theta \\ \text{or } c_d &= -\frac{1}{2} \int_0^{2\pi} C_p \cos \theta d\theta \end{aligned} \quad (3.130)$$

Substituting Equation (3.126) into (3.130), and noting that

$$\int_0^{2\pi} \cos \theta d\theta = 0 \quad (3.131a)$$

$$\int_0^{2\pi} \sin^2 \theta \cos \theta d\theta = 0 \quad (3.131b)$$

$$\int_0^{2\pi} \sin \theta \cos \theta d\theta = 0 \quad (3.131c)$$

we immediately obtain

$$c_d = 0 \quad (3.132)$$

Equation (3.132) confirms our intuitive statements made earlier. The drag on a cylinder in an inviscid, incompressible flow is zero, regardless of whether or not the flow has circulation about the cylinder.

The lift on the cylinder can be evaluated in a similar manner as follows. From Equation (1.15) with  $c_f = 0$ ,

$$c_l = c_n = \frac{1}{c} \int_0^c C_{p,l} dx - \frac{1}{c} \int_0^c C_{p,u} dx \quad (3.133)$$

Converting to polar coordinates, we obtain

$$x = R \cos \theta \quad dx = -R \sin \theta d\theta \quad (3.134)$$

Substituting Equation (3.134) into (3.133), we have

$$c_l = -\frac{1}{2} \int_{\pi}^{2\pi} C_{p,l} \sin \theta d\theta + \frac{1}{2} \int_{\pi}^0 C_{p,u} \sin \theta d\theta \quad (3.135)$$

Again, noting that  $C_{p,l}$  and  $C_{p,u}$  are both given by the same analytic expression, namely, Equation (3.126), Equation (3.135) becomes

$$c_l = -\frac{1}{2} \int_0^{2\pi} C_p \sin \theta d\theta \quad (3.136)$$

Substituting Equation (3.126) into (3.136), and noting that

$$\int_0^{2\pi} \sin \theta d\theta = 0 \quad (3.137a)$$

$$\int_0^{2\pi} \sin^3 \theta d\theta = 0 \quad (3.137b)$$

$$\int_0^{2\pi} \sin^2 \theta d\theta = \pi \quad (3.137c)$$

we immediately obtain

$$c_l = \frac{\Gamma}{RV_\infty} \quad (3.138)$$

From the definition of  $c_l$  (see Section 1.5), the lift per unit span  $L'$  can be obtained from

$$L' = q_\infty S c_l = \frac{1}{2} \rho_\infty V_\infty^2 S c_l \quad (3.139)$$

Here, the planform area  $S = 2R(1)$ . Therefore, combining Equations (3.138) and (3.139), we have

$$L' = \frac{1}{2} \rho_\infty V_\infty^2 2R \frac{\Gamma}{RV_\infty}$$

or

$$L' = \rho_\infty V_\infty \Gamma \quad (3.140)$$

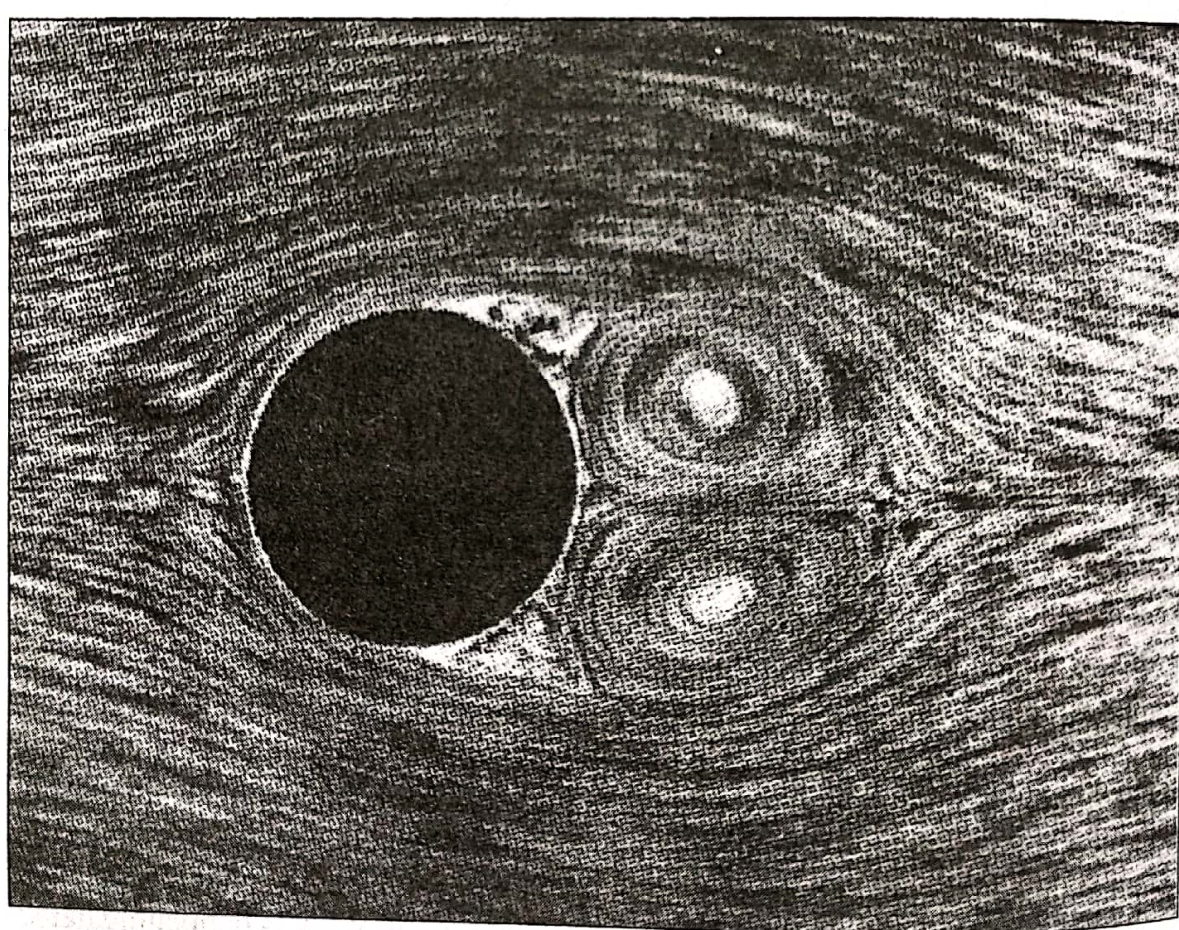
Equation (3.140) gives the lift per unit span for a circular cylinder with circulation  $\Gamma$ . It is a remarkably simple result, and it states that *the lift per unit span is directly proportional to circulation*. Equation (3.140) is a powerful relation in theoretical aerodynamics. It is called the *Kutta-Joukowski theorem*, named after the German mathematician M. Wilhelm Kutta (1867–1944) and the Russian physicist Nikolai E. Joukowski (1847–1921), who independently obtained it during the first decade of 20th century. We will have more to say about the Kutta-Joukowski theorem in Section 3.16.

What are the connections between the above theoretical results and real life? As stated earlier, the prediction of zero drag is totally erroneous—viscous effects cause skin friction and flow separation which always produce a finite drag. The inviscid flow treated in this chapter simply does not model the proper physics for drag calculations. On the other hand, the prediction of lift via Equation (3.140) is quite realistic. Let us return to the wind-tunnel experiments mentioned at the beginning of this chapter. If a stationary, nonspinning cylinder is placed in a low-speed wind tunnel, the flow field will appear as shown in Figure 3.34a. The streamlines over the front of the cylinder are similar to theoretical predictions, as sketched at the right of Figure 3.26. However, because of viscous effects, the flow separates over the rear of the cylinder, creating a recirculating flow in the wake downstream of the body. This separated flow greatly contributes to the finite drag measured for the cylinder. On the other hand, Figure 3.34a shows a reasonably symmetric flow about the horizontal axis, and the measurement of lift is essentially zero. Now let us *spin* the cylinder in a clockwise direction about its axis. The resulting flow fields are shown in Figure 3.34b and c. For a moderate amount of spin (Figure 3.34b), the stagnation points move to the lower part of the cylinder, similar to the theoretical flow sketched in Figure 3.33a. If the spin is sufficiently increased (Figure 3.34c), the stagnation point lifts off the surface, similar to the theoretical flow sketched in Figure 3.33c. And what is most important, a *finite lift* is measured for the spinning cylinder in the wind tunnel. What is happening here? Why does spinning the cylinder produce lift? In actuality, the friction between the fluid and the surface of the cylinder tends to drag the fluid near the surface in the same direction as the rotational motion. Superimposed on top of the usual nonspinning flow, this “extra” velocity contribution creates a higher-than-usual

velocity at the top of the cylinder and a lower-than-usual velocity at the bottom, as sketched in Figure 3.35. These velocities are assumed to be just outside the viscous boundary layer on the surface. Recall from Bernoulli's equation that as the velocity increases, the pressure decreases. Hence, from Figure 3.35, the pressure on the top of the cylinder is lower than on the bottom. This pressure imbalance creates a net upward force, that is, a finite lift. Therefore, the theoretical prediction embodied in Equation (3.140) that the flow over a circular cylinder can produce a finite lift is verified by experimental observation.

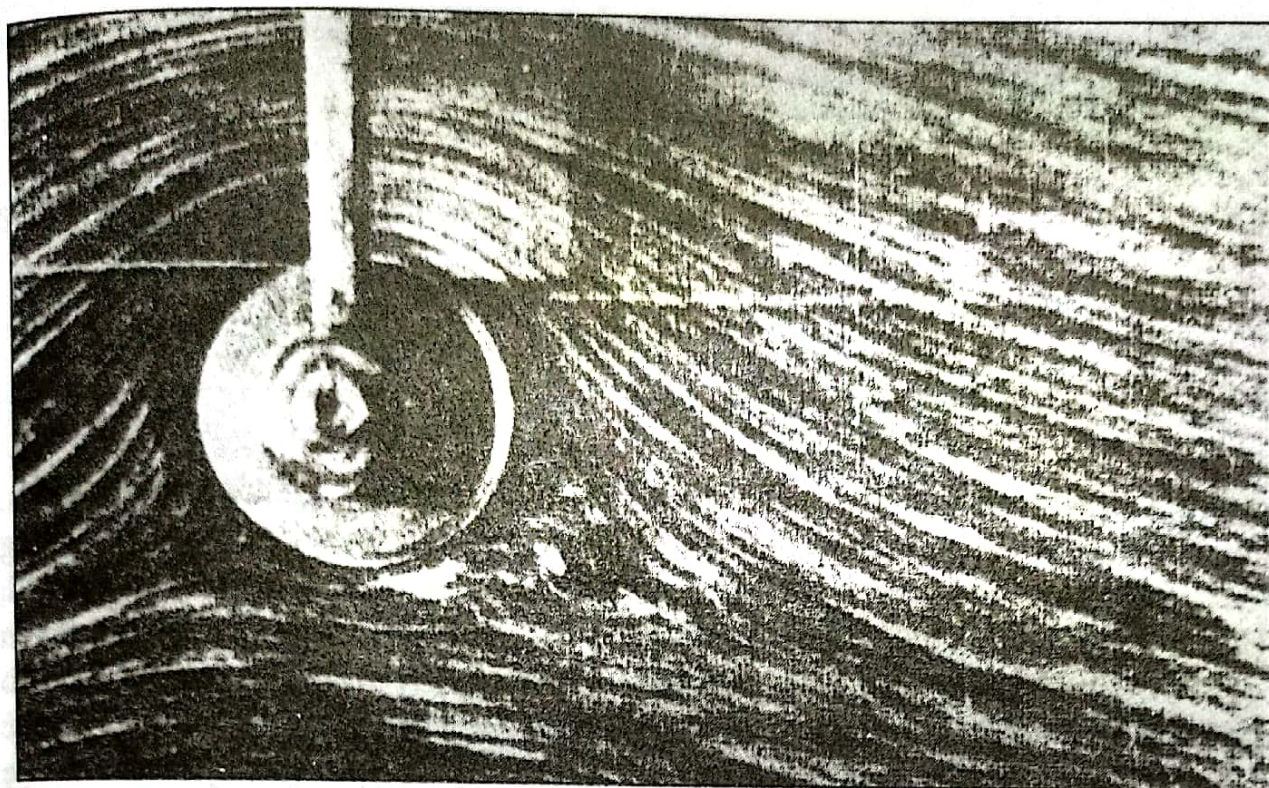
The general ideas discussed above concerning the generation of lift on a spinning circular cylinder in a wind tunnel also apply to a spinning sphere. This explains why a baseball pitcher can throw a curve and how a golfer can hit a hook or slice—all of which are due to nonsymmetric flows about the spinning bodies, and hence the generation of an aerodynamic force perpendicular to the body's angular velocity vector. This phenomenon is called the *Magnus effect*, named after the German engineer who first observed and explained it in Berlin in 1852.

It is interesting to note that a rapidly spinning cylinder can produce a much higher lift than an airplane wing of the same planform area; however, the drag on the cylinder is also much higher than a well-designed wing. As a result, the

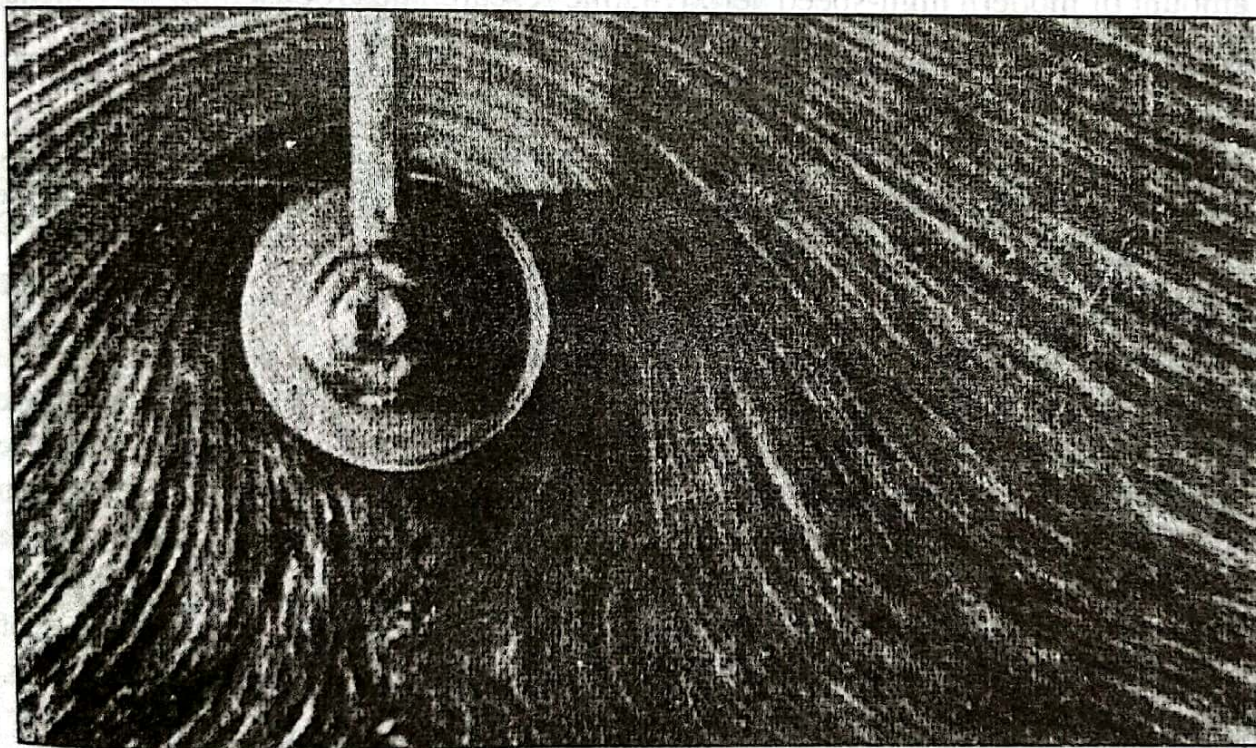


(a)

**Figure 3.34** These flow-field pictures were obtained in water, where aluminum filings were scattered on the surface to show the direction of the streamlines. (a) Shown above is the case for the nonspinning cylinder. (Source: Prandtl and Tietjens, Reference 8.)



(b)



(c)

**Figure 3.34** (continued) These flow-field pictures were obtained in water, where aluminum filings were scattered on the surface to show the direction of the streamlines. (b) Spinning cylinder: peripheral velocity of the surface =  $3V_\infty$ . (c) Spinning cylinder: peripheral velocity of the surface =  $6V_\infty$ . (Source: Prandtl and Tietjens, Reference 8.)

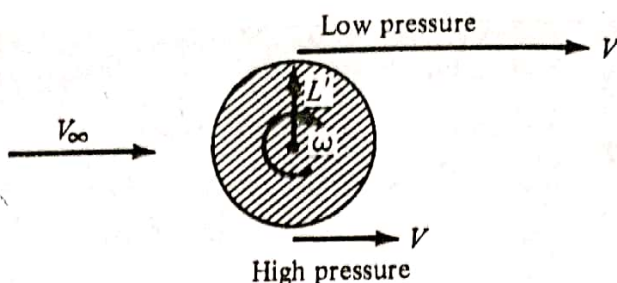


**Figure 3.35** Creation of lift on a spinning cylinder.

Magnus effect is not employed for powered flight. On the other hand, in the 1920s, the German engineer Anton Flettner replaced the sail on a boat with a rotating circular cylinder with its axis vertical to the deck. In combination with the wind, this spinning cylinder provided propulsion for the boat. Moreover, by the action of two cylinders in tandem and rotating in opposite directions, Flettner was able to turn the boat around. Flettner's device was a technical success, but an economic failure because the maintenance on the machinery to spin the cylinders at the necessary high rotational speeds was too costly. Today, the Magnus effect has an important influence on the performance of spinning missiles; indeed, a certain amount of modern high-speed aerodynamic research has focused on the Magnus forces on spinning bodies for missile applications.

#### EXAMPLE 3.14

Consider the lifting flow over a circular cylinder. The lift coefficient is 5. Calculate the peak (negative) pressure coefficient.

#### ■ Solution

Examining Figure 3.32, note that the maximum velocity for the *nonlifting* flow over a cylinder is  $2V_\infty$  and that it occurs at the top and bottom points on the cylinder. When the vortex in Figure 3.32 is added to the flow field, the direction of the vortex velocity is in the *same* direction as the flow on the top of the cylinder, but opposes the flow on the bottom of the cylinder. Hence, the maximum velocity for the lifting case occurs at the *top* of the cylinder and is equal to the sum of the nonlifting value,  $-2V_\infty$ , and the vortex,  $-\Gamma/2\pi R$ . (*Note:* We are still following the usual sign convention; since the velocity on the top of the cylinder is in the opposite direction of increasing  $\theta$  for the polar coordinate system, the velocity magnitudes here are negative.) Hence,

$$V = -2V_\infty - \frac{\Gamma}{2\pi R} \quad (E.1)$$

The lift coefficient and  $\Gamma$  are related through Equation (3.138):

$$c_l = \frac{\Gamma}{RV_\infty} = 5$$

Hence,

$$\frac{\Gamma}{R} = 5V_\infty \quad (E.2)$$

Substituting Equation (E.2) into (E.1), we have

$$V = -2V_\infty - \frac{5}{2\pi} V_\infty = -2.796 V_\infty \quad (\text{E.3})$$

Substituting Equation (E.3) into Equation (3.38), we obtain

$$C_p = 1 - \left( \frac{V}{V_\infty} \right)^2 = 1 - (2.796)^2 = \boxed{-6.82}$$

This example is designed in part to make the following point. Recall that, for an inviscid, incompressible flow, the distribution of  $C_p$  over the surface of a body depends only on the shape and orientation of the body—the flow properties such as velocity and density are irrelevant here. Recall Equation (3.101), which gives  $C_p$  as a function of  $\theta$  only, namely,  $C_p = 1 - 4 \sin^2 \theta$ . However, for the case of lifting flow, the distribution of  $C_p$  over the surface is a function of one additional parameter—namely, the lift coefficient. Clearly, in this example, only the value of  $c_l$  is given. However, this is powerful enough to define the flow uniquely; the value of  $C_p$  at any point on the surface follows directly from the value of lift coefficient, as demonstrated in the above problem.

### EXAMPLE 3.15

For the flow field in Example 3.14, calculate the location of the stagnation points and the points on the cylinder where the pressure equals freestream static pressure.

#### Solution

From Equation (3.123), the stagnation points are given by

$$\theta = \arcsin \left( -\frac{\Gamma c_l}{4\pi V_\infty R} \right)$$

From Example 3.14,

$$\frac{\Gamma c_l}{4\pi V_\infty R} = 5$$

$$\theta = \arcsin \left( -\frac{5}{4\pi} \right) = \boxed{203.4^\circ \text{ and } 336.6^\circ}$$

To find the locations where  $p = p_\infty$ , first construct a formula for the pressure coefficient on the cylinder surface:

$$C_p = 1 - \left( \frac{V}{V_\infty} \right)^2$$

$$V = -2V_\infty \sin \theta - \frac{\Gamma}{2\pi R}$$

where

**PART 2** Inviscid, Incompressible Flow

Thus,

$$C_p = 1 - \left( -2 \sin \theta - \frac{\Gamma}{2\pi R} \right)^2$$

$$= 1 - 4 \sin^2 \theta - \frac{2\Gamma \sin \theta}{\pi RV_\infty} - \left( \frac{\Gamma}{2\pi RV_\infty} \right)^2$$

From Example 3.14,  $\Gamma/RV_\infty = 5$ . Thus,

$$C_p = 1 - 4 \sin^2 \theta - \frac{10}{\pi} \sin \theta - \left( \frac{5}{2\pi} \right)^2$$

$$= 0.367 - 3.183 \sin \theta - 4 \sin^2 \theta$$

A check on this equation can be obtained by calculating  $C_p$  at  $\theta = 90^\circ$  and seeing if it agrees with the result obtained in Example 3.14. For  $\theta = 90^\circ$ , we have

$$C_p = 0.367 - 3.183 - 4 = \boxed{-6.82}$$

This is the same result as in Example 3.14; the equation checks.

To find the values of  $\theta$  where  $p = p_\infty$ , set  $C_p = 0$ :

$$0 = 0.367 - 3.183 \sin \theta - 4 \sin^2 \theta$$

From the quadratic formula,

$$\sin \theta = \frac{3.183 \pm \sqrt{(3.183)^2 + 5.872}}{-8} = \boxed{-0.897 \text{ or } 0.102}$$

Hence,

$$\theta = 243.8^\circ \text{ and } 296.23^\circ$$

Also,

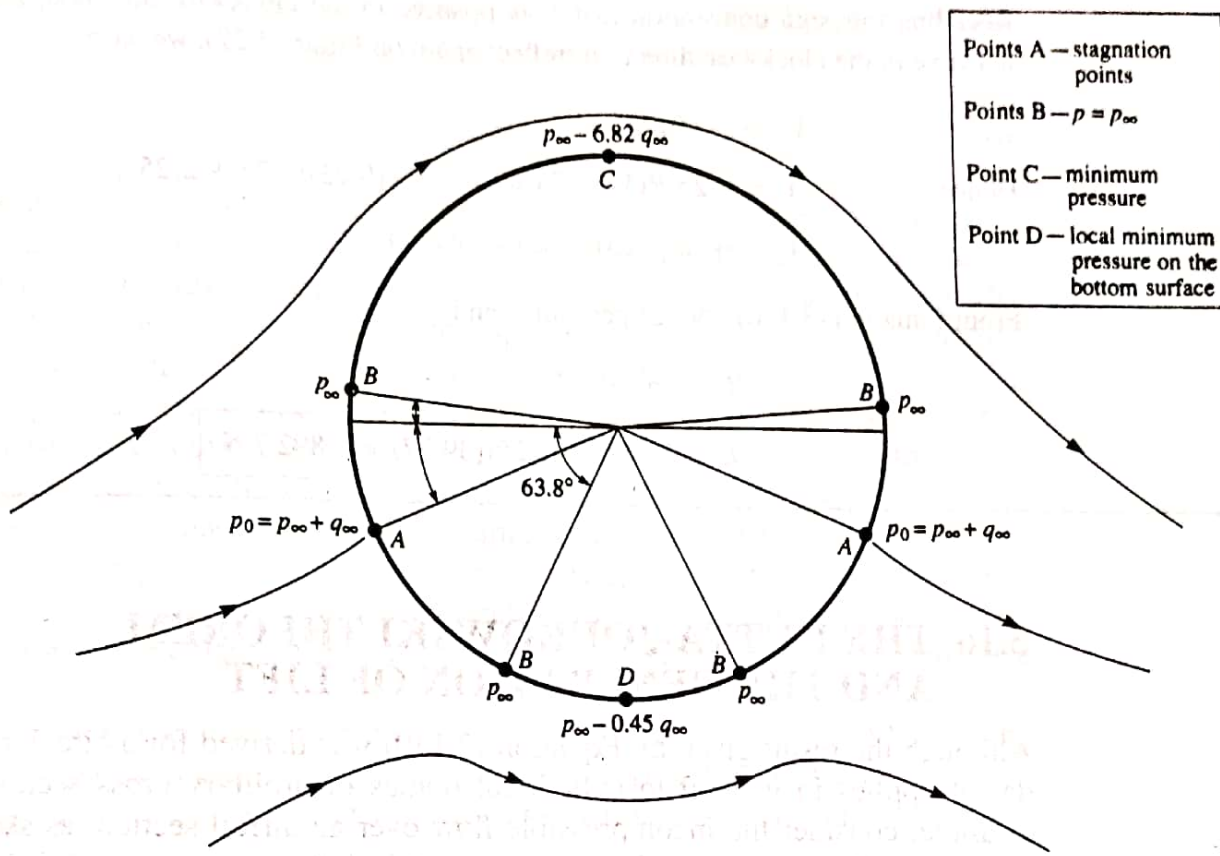
$$\theta = 5.85^\circ \text{ and } 174.1^\circ$$

There are four points on the circular cylinder where  $p = p_\infty$ . These are sketched in Figure 3.36, along with the stagnation point locations. As shown in Example 3.14, the minimum pressure occurs at the top of the cylinder and is equal to  $p_\infty - 6.82q_\infty$ . A local minimum pressure occurs at the bottom of the cylinder, where  $\theta = 3\pi/2$ . This local minimum is given by

$$C_p = 0.367 - 3.183 \sin \frac{3\pi}{2} - 4 \sin^2 \frac{3\pi}{2}$$

$$= 0.367 + 3.183 - 4 = \boxed{-0.45}$$

Hence, at the bottom of the cylinder,  $p = p_\infty - 0.45q_\infty$ .



- Points A — stagnation points
- Points B —  $p = p_\infty$
- Point C — minimum pressure
- Point D — local minimum pressure on the bottom surface

**Figure 3.36** Values of pressure at various locations on the surface of a circular cylinder; lifting case with finite circulation. The values of pressure correspond to the case discussed in Example 3.15.

#### EXAMPLE 3.16

Consider the lifting flow over a circular cylinder with a diameter of 0.5 m. The freestream velocity is 25 m/s, and the maximum velocity on the surface of the cylinder is 75 m/s. The freestream conditions are those for a standard altitude of 3 km. Calculate the lift per unit span on the cylinder.

#### Solution

From Appendix D, at an altitude of 3 km,  $\rho = 0.90926 \text{ kg/m}^3$ . The maximum velocity occurs at the top of the cylinder, where  $\theta = 90^\circ$ . From Equation (3.125),

$$V_\theta = -2V_\infty \sin \theta - \frac{\Gamma}{2\pi R}$$

At  $\theta = 90^\circ$

$$V_\theta = -2V_\infty - \frac{\Gamma}{2\pi R}$$

or,

$$\Gamma = -2\pi R(V_\theta + 2V_\infty)$$

Recalling our sign convention that  $\Gamma$  is positive in the clockwise direction, and  $V_\theta$  is negative in the clockwise direction (reflect again on Figure 3.32), we have

$$V_\theta = -75 \text{ m/s}$$

Hence,

$$\Gamma = -2\pi R(V_\theta + 2V_\infty) = -2\pi(0.25)[-75 + 2(25)]$$

$$\Gamma = -2\pi(0.25)(-25) = 39.27 \text{ m}^2/\text{s}$$

From Equation (3.140), the lift per unit span is

$$L' = \rho_\infty V_\infty \Gamma$$

$$L' = (0.90926)(25)(39.27) = \boxed{892.7 \text{ N}}$$

### 3.16 THE KUTTA-JOUKOWSKI THEOREM AND THE GENERATION OF LIFT

Although the result given by Equation (3.140) was derived for a circular cylinder, it applies in general to cylindrical bodies of arbitrary cross section. For example, consider the incompressible flow over an airfoil section, as sketched in Figure 3.37. Let curve  $A$  be any curve in the flow enclosing the airfoil. If the airfoil is producing lift, the velocity field around the airfoil will be such that the line integral of velocity around  $A$  will be finite, that is, the circulation

$$\Gamma \equiv \oint_A \mathbf{V} \cdot d\mathbf{s}$$

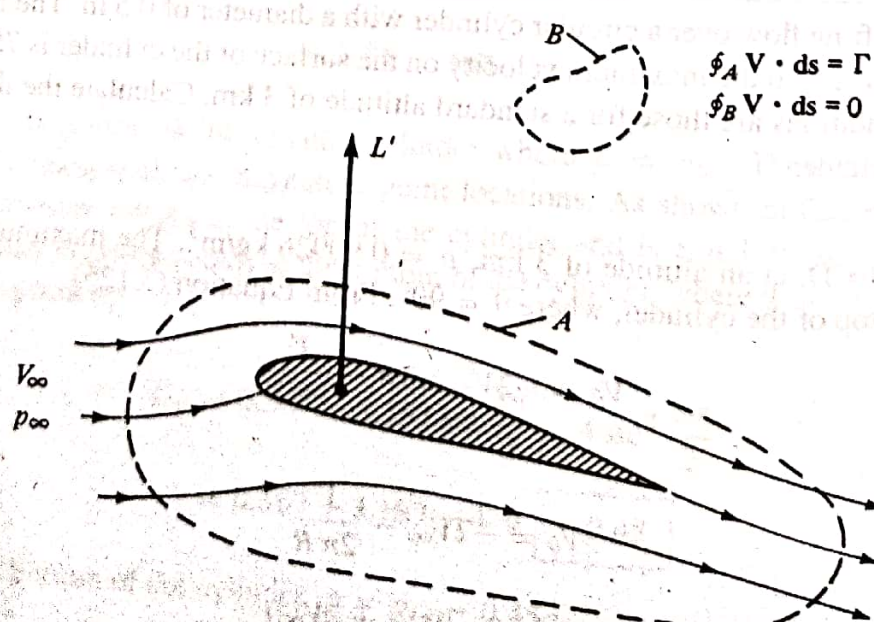


Figure 3.37 Circulation around a lifting airfoil.

is finite. In turn, the lift per unit span  $L'$  on the airfoil will be given by the *Kutta-Joukowski theorem*, as embodied in Equation (3.140):

$$L' = \rho_\infty V_\infty \Gamma \quad (3.140)$$

This result underscores the importance of the concept of circulation, defined in Section 2.13. The Kutta-Joukowski theorem states that lift per unit span on a two-dimensional body is directly proportional to the circulation around the body. Indeed, the concept of circulation is so important at this stage of our discussion that you should reread Section 2.13 before proceeding further.

The general derivation of Equation (3.140) for bodies of arbitrary cross section can be carried out using the method of complex variables. Such mathematics is beyond the scope of this book. (It can be shown that arbitrary functions of complex variables are general solutions of Laplace's equation, which in turn governs incompressible potential flow. Hence, more advanced treatments of such flows utilize the mathematics of complex variables as an important tool. See Reference 9 for a particularly lucid treatment of inviscid, incompressible flow at a more advanced level.)

In Section 3.15, the lifting flow over a circular cylinder was synthesized by superimposing a uniform flow, a doublet, and a vortex. Recall that all three elementary flows are irrotational at all points, except for the vortex, which has infinite vorticity at the origin. Therefore, the lifting flow over a cylinder as shown in Figure 3.33 is irrotational at every point except at the origin. If we take the circulation around any curve *not* enclosing the origin, we obtain from Equation (2.137) the result that  $\Gamma = 0$ . It is only when we choose a curve that encloses the origin, where  $\nabla \times \mathbf{V}$  is infinite, that Equation (2.137) yields a finite  $\Gamma$ , equal to the strength of the vortex. The same can be said about the flow over the airfoil in Figure 3.37. As we show in Chapter 4, the flow *outside* the airfoil is irrotational, and the circulation around any closed curve *not* enclosing the airfoil (such as curve *B* in Figure 3.37) is consequently zero. On the other hand, we also show in Chapter 4 that the flow over an airfoil is synthesized by distributing vortices either on the surface or inside the airfoil. These vortices have the usual singularities in  $\nabla \times \mathbf{V}$ , and therefore, if we choose a curve that encloses the airfoil (such as curve *A* in Figure 3.37), Equation (2.137) yields a finite value of  $\Gamma$ , equal to the *sum* of the vortex strengths distributed on or inside the airfoil. The important point here is that, in the Kutta-Joukowski theorem, the value of  $\Gamma$  used in Equation (3.140) must be evaluated around a closed curve that *encloses the body*; the curve can be otherwise arbitrary, but it must have the body inside it.

At this stage, let us pause and assess our thoughts. The approach we have discussed above—the definition of circulation and the use of Equation (3.140) to obtain the lift—is the essence of the *circulation theory of lift* in aerodynamics. Its development at the turn of the twentieth century created a breakthrough in aerodynamics. However, let us keep things in perspective. The circulation theory of lift is an *alternative* way of thinking about the generation of lift on an aerodynamic body. Keep in mind that the true physical sources of aerodynamic force

on a body are the pressure and shear stress distributions exerted on the surface of the body, as explained in Section 1.5. The Kutta-Joukowski theorem is simply an alternative way of expressing the *consequences* of the surface pressure distribution; it is a mathematical expression that is consistent with the special tools we have developed for the analysis of inviscid, incompressible flow. Indeed, recall that Equation (3.140) was derived in Section 3.15 by integrating the pressure distribution over the surface. Therefore, it is not quite proper to say that circulation “causes” lift. Rather, lift is “caused” by the net imbalance of the surface pressure distribution, and circulation is simply a defined quantity determined from the same pressures. The relation between the surface pressure distribution (which produces lift  $L'$ ) and circulation is given by Equation (3.140). However, in the theory of incompressible, potential flow, it is generally much easier to determine the circulation around the body rather than calculate the detailed surface pressure distribution. Therein lies the power of the circulation theory of lift.

Consequently, the theoretical analysis of lift on two-dimensional bodies in incompressible, inviscid flow focuses on the calculation of the circulation about the body. Once  $\Gamma$  is obtained, then the lift per unit span follows directly from the Kutta-Joukowski theorem. As a result, in subsequent sections we constantly address the question: How can we calculate the circulation for a given body in a given incompressible, inviscid flow?

### 3.17 NONLIFTING FLOWS OVER ARBITRARY BODIES: THE NUMERICAL SOURCE PANEL METHOD

In this section, we return to the consideration of nonlifting flows. Recall that we have already dealt with the nonlifting flows over a semi-infinite body and a Rankine oval and both the nonlifting and the lifting flows over a circular cylinder. For those cases, we added our elementary flows in certain ways and discovered that the dividing streamlines turned out to fit the shapes of such special bodies. However, this indirect method of starting with a given combination of elementary flows and seeing what body shape comes out of it can hardly be used in a practical sense for bodies of arbitrary shape. For example, consider the airfoil in Figure 3.37. Do we know in advance the correct combination of elementary flows to synthesize the flow over this specified body? The answer is no. Rather, what we want is a direct method; that is, let us *specify* the shape of an arbitrary body and *solve* for the distribution of singularities which, in combination with a uniform stream, produce the flow over the given body. The purpose of this section is to present such a direct method, limited for the present to nonlifting flows. We consider a numerical method appropriate for solution on a high-speed digital computer. The technique is called the *source panel method*, which, since the late 1960s, has become a standard aerodynamic tool in industry and most research laboratories. In fact, the numerical solution of potential flows by both source and vortex panel techniques has revolutionized the analysis of low-speed flows. We return to various numerical panel techniques in Chapters 4 through 6. As a modern study